DOI: http://dx.doi.org/10.32571/ijct.1507097 **E-ISSN: 2602-277X**

International Journal of Chemistry and Technology

http://dergipark.org.tr/ijct

Research Article

Easy and eco-friendly way for silver nanoparticles synthesis using *Lotus corniculatus L*: characterization and antibacterial activity

Assia BESSI [1]*, Hamza KAHINA[1,2], Boubkeur BOUDINE [3], Chaouki BOUDAREN [4]

[1]*Laboratoire de chimie physique moleculaire et macromoleculaire LCPMM , Saad Dahleb University, Route Soumâa BP 270, Blida 09000 , Algeria.*

[2]*Laboratoire de recherche sur les produits bioactifs et la valorisation de la biomasse(LPBVB) ; ENS Kouba, Algiers16000, Algeria..*

[3]*Crystallography Laboratory, Physics Department, Faculty of Exact Sciences, Mentouri Brothers University, Route Ain El Bey, Constantine 25000, Algeria.*

[4]*CHEMS Research Unit, Mentouri Brothers University, Route Ain El Bey, Constantine 25000, Algeria.*

Received: 1 July 2024; Revised: 8 December 2024; Accepted: 9 December 2024

*****Corresponding author e-mail: asieadz@yahoo.fr

Citation: Bessi, A.; Kahina, H.; Boudine, B; Boudaren, C. *Int. J. Chem. Technol.* **2024**, 8(2), 180-189.

ABSTRACT

Lotus corniculatus L. is a plant that has recently proven a significant effect in anticancer therapies. On the other side, silver nanoparticles have always proven to demonstrate pronounced antimicrobial and anti-inflammatory properties. To harness the collective advantages of both entities, we synthesized silver nanoparticles using an aqueous extract of *Lotus corniculatus L*. In this synthesis, we used a solution of $AgNO_3$ as a precursor of Ag, while existing bioactive molecules in the extract acted as a reducing agent and natural stabilizer of formed nanoparticles.

Structural characterization of the product was done by X-ray diffractometry (XRD) and infrared spectroscopy (FT-IR). Scanning electron microscopy with energy dispersive X-rays (SEM with EDX) was used to investigate nanoparticles morphology, and optical characterization was completed by Ultraviolet-visible spectrophotometry (UV-Vis).
An absorption edge at 420 nm and a noticeable color shift in the extract following the addition of the precursor demonstrated the AgNPs formation. SEM verified that the nanoparticles were spherical and had an average size of 17 nm. Importantly, the synthesized nanoparticles displayed an important antimicrobial activity, which is exhibited more remappable counter to gram-negative (*Escherichia coli*, *Pseudomonas aeruginosa)* than gram-positive (*Bacillus subtilis*). These findings underscore the potential of the *Lotus corniculatus L*. extract in silver nanoparticles synthesis as a promising avenue for applications in medicine and antimicrobial therapies.

Keywords: *Lotus corniculatus L*, green synthesis, silver nanoparticles, antibacterial activity.

1. INTRODUCTION

In recent years, there has been a burgeoning and fervent interest in all things related to "nanotechnologies." Researchers have enthusiastically embraced this interdisciplinary field, combining art and science to manipulate materials at the nanoscale through the integration of molecules, thus producing nano-objects via nanoscience. The exploration of nanoscale phenomena holds great promise for advancements in various domains, including chemistry[1], physics,[2] biology,[3] environmental science[4] and diverse sectors like electronics, food and notably, medicine,[5-7] particularly in anticancer therapies, is grounded in their

DOI: http://dx.doi.org/10.32571/ijct.1507097 E-ISSN: 2602-277X

ability to interact with biological entities, enabling targeted drug delivery and therapeutic interventions[8].

A material can be described as nanoscale when it has external dimensions or an internal or surface structure at the nanoscale. This size range is approximately 1 to 100 nm. nanomaterials, consisting of particles in an unbound state, as well as aggregates or agglomerates. For at least 50% of the particles in the particle size distribution, one or more external dimensions fall within the size range of 1 to 100 nm. They are distinguished by their significantly enhanced specific surface area, which leads to improved physical and chemical properties compared to bulk materials. These unique properties are due to their high surface/volume ratio, which determines their optical, mechanical, and electronic properties. Thus, nanoparticles have become a focal point of researchers' attention [9]

Nanoparticles can be made of metals, metal oxides, polymers and others, and they are used in many branches like medicine, electronics, energy, and environment. Noble metals, specifically gold and silver nanoparticles, occupy a key position in scientific investigations due to their unique optical, electrical, and catalytic properties, as well as their potential for applications in sensing, biomedical imaging, and therapeutics.[10-11]

Silver has held historical significance dating back to ancient times, with a perceived mysticism associated with its purported ability to remedy various ailments. This reverence stemmed from a belief in its inherent healing properties and an attribution of a protective quality against malevolent forces. The persistent cultural and historical veneration of silver endured until advancements in scientific understanding facilitated a comprehensive explanation for the distinctive properties associated with silver. In essence, the historical reverence for silver finds validation in its scientifically substantiated properties, where antimicrobial efficacy and the distinct characteristics of silver nanoparticles contribute to its continued relevance in modern applications and therapeutic endeavors.

Metallic silver nanoparticles (AgNPs) have played a considerable role in several fields because of their potential applications, especially in antimicrobial, antifungal, anti-proliferative and biomedical applications which are replicated in recent inventions.[12-14]

The silver nanoparticles in recent studies showed that they can be used as antitumor agents[15] because of their apoptotic and necrotic effect.[16] The researchers found that the anticancer activity of AgNPs is controlled via physicochemical properties like: size, charge of the surface, and molecules coating nanoparticles.

Typically, nanoparticles are prepared using physical or chemical processes. However, the chemicals employed in these methods are often costly, harmful, and flammable. Green synthesis, on the other hand, represents an eco-friendly, rapid, low-cost, and energy-conserving alternative for nanoparticle preparation. This approach seeks to harness the benefits of nanoparticles while simultaneously avoiding adverse environmental effects[17].

Used in traditional medicine, medicinal plants are recognized for their useful effects and healing properties. Now, their efficacy is scientifically proven, principally due to their strong antioxidant, antimicrobial, and antibacterial activities. All parts of medicinal plants as leaves, flowers, roots, fruits, and seeds can be used directly or incorporated into medicines, cosmetics, and agri-food products. Previous works reported the development AgNPs from a variety of plant sources. A pioneering report by Jorge L. Gardea-Torresdey *et al*[18] demonstrated the synthesis of silver by *living alfalfa* plants. The study revealed the formation of nanoparticle arrangements within *alfalfa* plant tissues due to the accumulation of silver atoms. After this work, a biological elaboration of silver nanoparticles using leaching dried *Cinnamomum camphora* leaves in continuous flow tubular microreactors was done by kung Huang *et al*[19] . This study supposed that polyols exist in the *lixivium* reduce silver ions to silver NPs. In 2010 Naheed Ahmad *et al* used a single, environmentally friendly step to synthesize silver nanoparticles from *Desmodium triflorum*. Their study highlighted the role of H^+ ions and NAD, as well as water-soluble antioxidants in plants, acting as redoxing agents, explaining the formation of Ag NPs[20] .Another investigation by S. Kaviya *et al* utilized *Citrus Sinensis* peels for silver nanoparticle synthesis, concluding that peel extracts functioned as both capping and reducing agents, producing spherical nanoparticles. The size of NPs is related to the synthesis reaction temperature and the resulting NPs have a good antibacterial activity[21]. Although several plants were used for (AgNPs) synthesis by a simple process, but there is still a necessity to develop improved approaches based on green nanotechnology. In order to supplement an environmentally and economically sound as well as commercially viable approach to synthesizing NPs and simultaneously try to increase the relevancy of available drugs and antiviral/antimicrobial materials. Given these considerations, the plant chosen for this research is *Lotus corniculatus*, commonly known as Bird's-foot trefoil, is a perennial herbaceous plant of the Fabaceae family. It is cultivated as a forage plant. The trefoil is commonly known as hounds tooth, pretty pea, bride's shoe, is a low plant, rather lying down, leaves with three oval leaflets, the stipules located at the base being similar. The plant has solid stems, which help distinguish it from another common trefoil species. Its

DOI: http://dx.doi.org/10.32571/ijct.1507097 E-ISSN: 2602-277X

flowers are typically bright yellow or yellow-orange and are grouped in small, rounded clusters .This plant is recognized for its therapeutic properties, including anti-inflammatory and antioxidant effects,[22] hepatoprotective agent,[23] and more recently, its application in seizures treatment,[24] and more recently, its application in seizures treatment. Several phytochemical compounds, including flavonoids, phenolic acids, saponins, and condensed tannins, have been identified in various parts of *Lotus* species.[17, 25-27]Additionally, investigations into the aerial parts of the plant have revealed compounds such as benzoic acid, p-coumaric acid, phenolic glucoside, a flavonoid, saponins, glycosides, and transilin.[28,29] These compounds, rich in diverse chemical functionalities, tend out as effective capping agents in the biosynthesis of silver nanoparticles. The adoption of water in aqueous extracts, as opposed to toxic reducing agents and expensive solvents, aligns with the principles of green chemistry.[30] However, despite the existing knowledge on Lotus species and their phytochemical composition, there is a conspicuous absence of information regarding the use of *Lotus corniculatus L* in the green synthesis of nanomaterials in prior studies. This notable gap serves as the impetus for our current work, wherein we aim to assess the potential of *Lotus corniculatus L*, abundantly found in Algeria, for the biosynthesis of metallic nanoparticles. Our approach integrates the documented anticancer properties of *L. corniculatus* with the well-established antimicrobial and anti-inflammatory attributes of silver nanoparticles. By leveraging the synergistic effects of these properties, we strive to develop a novel material with enhanced therapeutic potential. This exploration of *L. corniculatus* in the context of metallic nanoparticle biosynthesis represents a novel avenue in nanomaterial research and seeks to fill an existing void in the current scientific understanding.

2. MATERIALS AND METHODS

2.1. Materials

All solvents and chemicals used in silver nanoparticles synthesis and antibacterial activity tests were obtained from Sigma Aldrich Germany.

The *Lotus corniculatus*, aerial parts were collected in March 2021 from Constantine located in the Eastern region of Algeria. Following collection, the plant was air-dried in the shade at room temperature (25°C) for a period of one week.

2.2. Methods

2.2.1. Silver Nanoparticles Synthesis

30 g of the dried plant material were mixed with (200 mL) of deionized water and stirred at a temperature of 60°C for a duration of 4 hours. The resulting extract underwent filtration and was then stored at a temperature of 4°C.

In typical experiment, (20 mL of 10^{-3} M) $AgNO_3$ solution was gradually added dropwise to 10 mL of the aqueous plant extract. This mixture was stirred overnight in a dark chamber to minimize the potential for photoactivation of silver nitrate. Throughout this process, a noticeable color change (to brown) occurred, and a precipitate formed, as depicted in (Figure 1). The solid phase obtained was subsequently dried and subjected to calcination for a duration of 2 hours at 400°C.

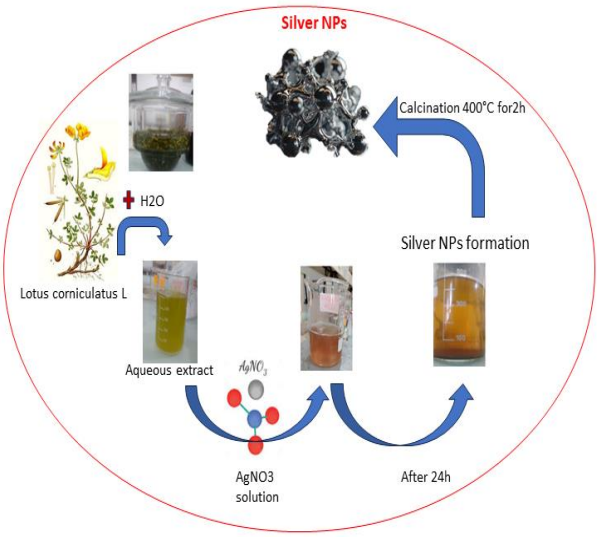

Figure 1. Photographs of silver nanoparticles green synthesis process.

2.2.2. Characterization of Silver Nanoparticles

The identification of prepared samples phase was made via a Burker Phaser powder diffractometer (λ_{Cu} (Kα) = 1.54 ° A), basing on Scherrer equation (1) to estimate the nanoparticles average size.

$$d = \frac{0.9\lambda}{\beta \cos(\theta)} \quad (1)$$

(*d*): size of particles (nm), (λ): X-ray wavelengths (1.54 Å), *(β)*: (FWHM) and *(θ)*:Bragg angle (degree).

The FTIR samples spectra were registered in transmission mode via JASCO FTIR 4100 spectrophotometer in KBr pellets.

A Varian-Cary system 500 UV–Vis spectrophotometer was utilized to define the optical properties (UV–Vis absorption) of AgNPs at room temperature.

The morphology of the product was attained via a field emission scanning electron microscopy (SEM Quanta 250), finally the chemical analysis of product was

DOI: http://dx.doi.org/10.32571/ijct.1507097 E-ISSN: 2602-277X

carried out with Energy-dispersive X-ray analysis (EDX).

2.2.3. Procedure of Antibacterial Activity

The antibacterial assays were done using standard disc diffusion method on gram negative *Escherichia coli*, *Pseudomonas aeruginosa* and gram-positive *Bacillus subtilis*. The plates were cultured by adding (20 mL) of Muller-Hinton agar, which was then buffered with *B. subtilis*, *E. coli* and *P. aeruginosa* isolates. Sterile 5 mm diameter discs loaded with AgNPs suspensions with various concentrations were made, ((2, 4, 6, 8 and 10)*10^2 µg/mL by dissolving in dimethyl sulfoxide (DMSO)) then inserted in separately plate and incubated for 24 h at 37°C. The existence of inhibitory zones surrounding discs revealed antibacterial activity. At the end of the development period, the zones of inhibition diameters were measured in mm.

3. RESULTS AND DISCUSSION

3.1. X-ray Diffraction (XRD)

To investigate the composition and the structure of elaborated powder, we use the XRD diffraction. Figure 2 shows a cubic face centered crystal structure for synthesized Ag NPs compared to the (JCPDS N°:04–0783).[31] Silver NPs specific diffraction peaks were detected at 37.75°, 45.°, 64, and 67.5° of 2θ values attributed to reflection from (111), (200), (220) and (311) crystal facet respectively.[32] We found also other peaks at 28.2°, 29.1° and 31° of 2θ values, which are designated by stars, the same peaks were found in other studies , the presence of these peaks is justified by probable interaction between silver nitrate and biologic lattice or by mineral complexes formation such as Ag_3PO_4.[33] The average crystallite size calculated using Sherre's formula is found to be 17 nm.

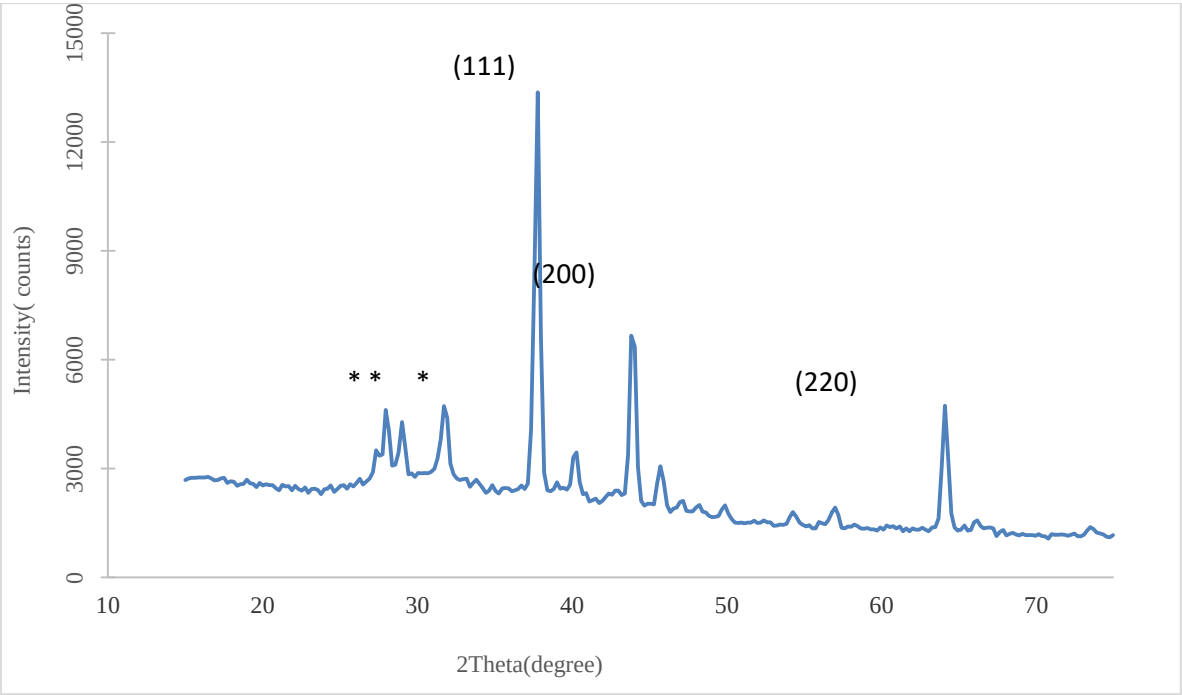

Figure 2. XRD pattern of AgNP.

3.2. UV-Vis Spectroscopy Investigation

The discernible change in the color of the extract provides clear confirmation of the successful formation of silver nanoparticles (Ag NPs) through the reduction of Ag^+ to Ag^0.[34,35] As extensively documented in previous studies, the intricate interplay of proteins, flavonoids, polyphenols, and other secondary metabolites within the extract is integral to the dual role they play as both reducing and capping agents. Proteins and polyphenols, in particular, exhibit a propensity to donate electrons, facilitating the reduction of Ag^+ ions, while flavonoids and other secondary metabolites act as stabilizing agents, preventing agglomeration and ensuring stability of the synthesized AgNPs.[36] Examining the UV-Vis spectra presented in (Figure 3), the distinct plasmon band of the Ag NPs suspension is evident, showcasing a well-defined absorption peak around 420 nm. This peak corresponds to the characteristic surface plasmon resonance (SPR) of the nanoparticles, a phenomenon commonly observed in metallic nanomaterials.[37] The uniformity of these results with other studies utilizing the same $AgNO_3$ concentration as the work of D. Jain *et al* [38] , Erenler, R

DOI: http://dx.doi.org/10.32571/ijct.1507097 E-ISSN: 2602-277X

et al[39] with minor variations, reinforces the reproducibility and reliability of the synthesis process. An intriguing aspect worth noting is the observed blue shift in the absorption peak, attributable to the quantum size effect. This phenomenon underscores the unique optical properties of nanoscale materials, wherein confinement of electrons within the smaller nanoparticle size leads to alterations in their electronic structure. In this context, the blue shift in plasmon energies indicates the quantum size effects in the synthesized Ag NPs compared to larger Ag massif crystals.[40-42] This nuanced understanding of the optical behavior adds depth to our interpretation, emphasizing the importance of considering quantum size effects in the synthesis and characterization of silver nanoparticles.

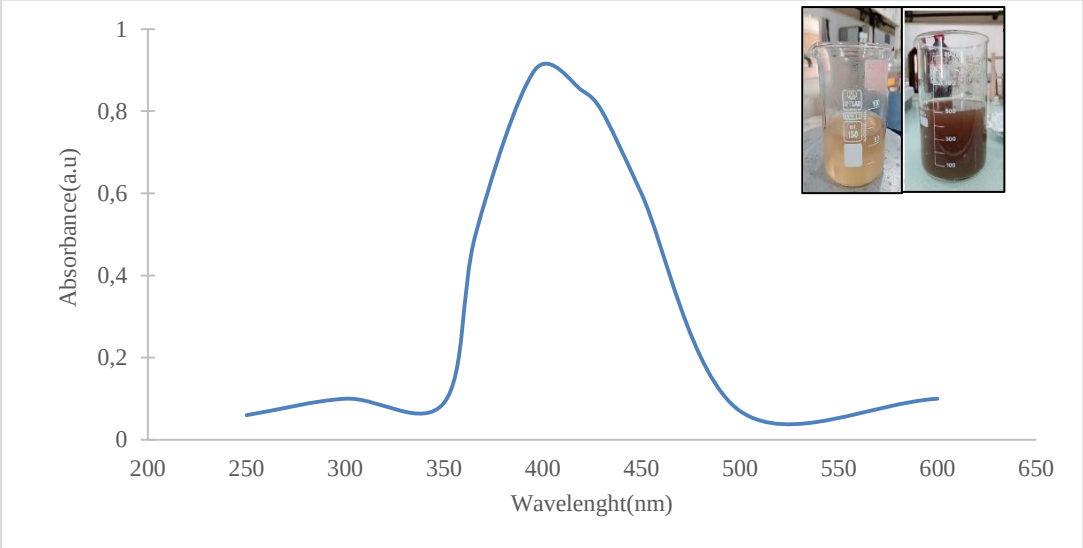

Figure 3.UV-Vis spectrum of biosynthesized silver NPs.

3.3. Fourier Transform Infra-Red (FTIR) Spectroscopy

The FT-IR analysis is utilized to define the functional groups existing in the aqueous extract probably responsible for production and stabilizing AgNPs.

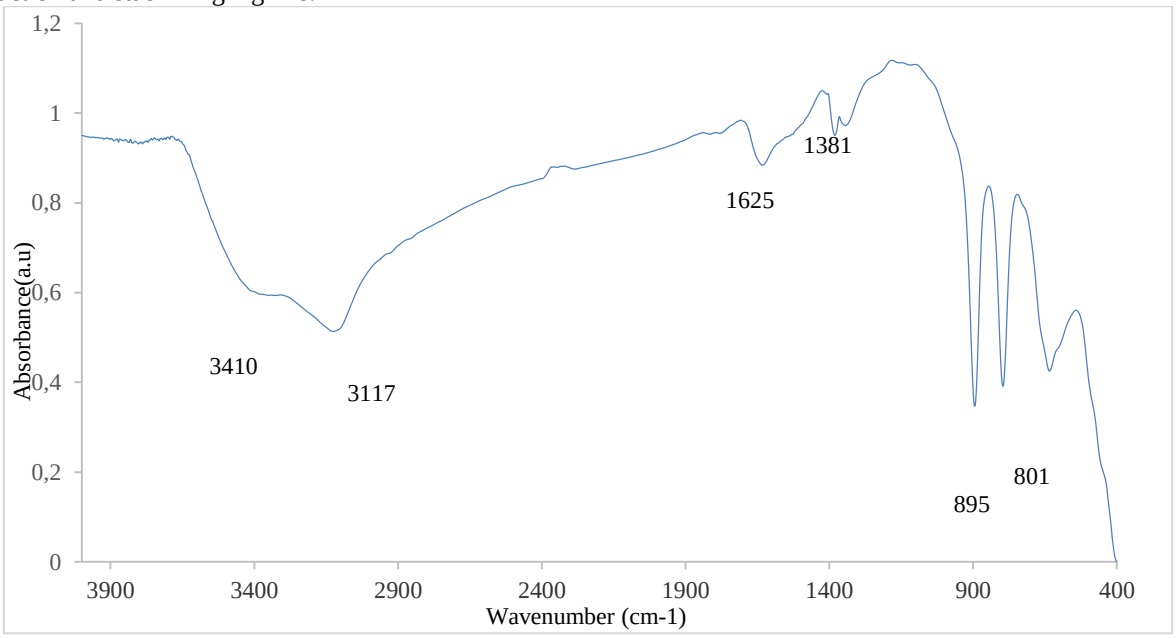

Figure 4. IRFT of biosynthesized AgNPs.

DOI: http://dx.doi.org/10.32571/ijct.1507097 E-ISSN: 2602-277X

As shown in (Figure 4), the broad and strong bands at 3410 attributed to the vibration of O-H groups of polyphenolics or flavonoids. Additionally, absorption peaks at 1626 and 1381 cm^{-1} assigned to C=O stretching, while the band at 3117 cm^{-1} are probably due to the presence of amide function I and II respectively.[43] Notably, the bands at 895 and 801 cm^{-1} are attributed to deformation vibration = C-H out of plane.[44]

These FTIR results confirmed the presence of different bioactive molecules within the aqueous extract of *L. corniculatus*, with notable constituents such as flavonoids and polyphenols which participate in the reduction of silver nitrate, and therefore the biosynthesis of AgNPs.

The synthesis mechanism proposed for AgNPs formation in this process involves the reduction of Ag^+ to Ag^0 facilitated by secondary metabolic reactions.[45]

$$2Ag^+ + 2e^- \longrightarrow 2Ag^0$$

Or

$$2H^+ + 2e^- \longrightarrow H_2$$

$$2Ag^+ + H_2 \longrightarrow 2Ag^0 + 2H^+$$

This mechanism (Figure 5) underscores the intricate interplay between the bioactive components in the plant extract and their pivotal role in the successful fabrication of silver nanoparticles.

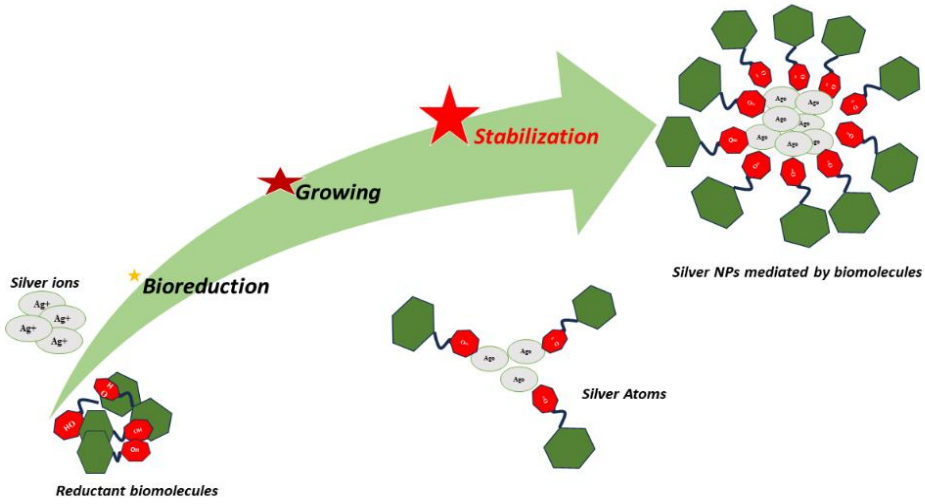

Figure 5. Mechanism steps of Silver NPs green synthesis.

3.4. Scanning Electronic Microscope -Energy Dispersive X-ray Spectroscopy (SEM-EDX) Analysis

The SEM micrographs presented in (Figure 6(a)) clearly illustrate the spherical shape of the synthesized nanoparticles. Especially with nanometric size (Figure 6(c)) highlighting the uniformity and consistency achieved in the synthesis process. On the EDX (Figure 6(b)), distinctive silver optical absorption band peak is clearly visible in the spectrum at around 3KeV.[46,47] This unique peak attests to the effective synthesis of AgNPs by confirming the presence of silver nanoparticles. The EDX spectrum also shows the presence of other metal peaks, indicating that there might be more components coming from the plant extract. This careful examination suggests that the intricate interactions among the plant's bioactive chemicals during the creation of the nanoparticles may be responsible for the distinct features and attributes of the final product. The EDX results, therefore, provide a comprehensive understanding of the elemental composition, further enriching our comprehension of the synthesized AgNPs.

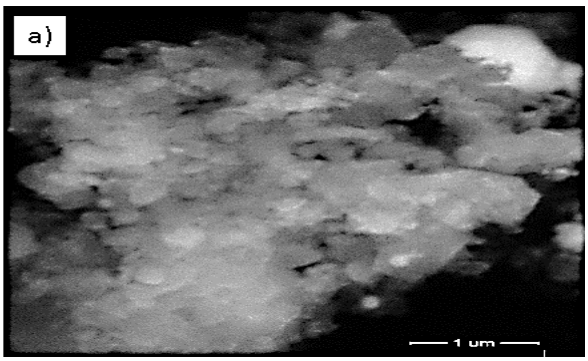

DOI: http://dx.doi.org/10.32571/ijct.1507097 E-ISSN: 2602-277X

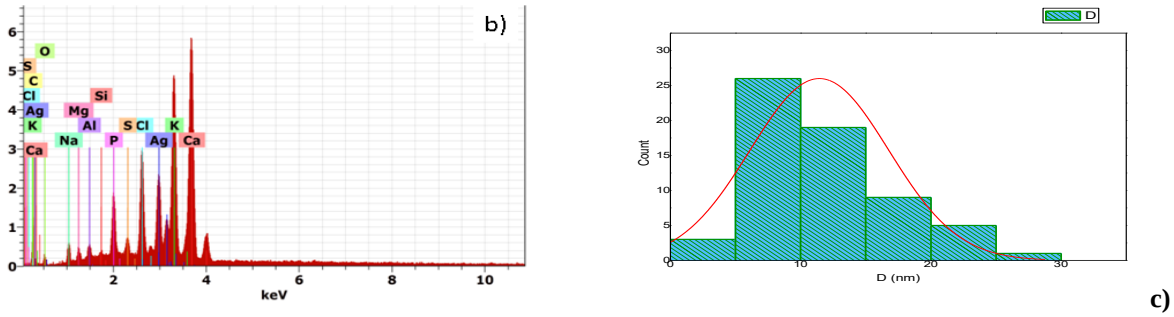

Figure 6. a) ,b) and c) Scanning Electron Microscope: a) Ag NPs micrographs, b) EDX of biosynthesized AgNPs, c) Particles size distribution.

3.5. Antimicrobial Activity

The inhibition zone of bacterial growth around each sample shown in (Figure 7) was measured and summarized in Table 1.

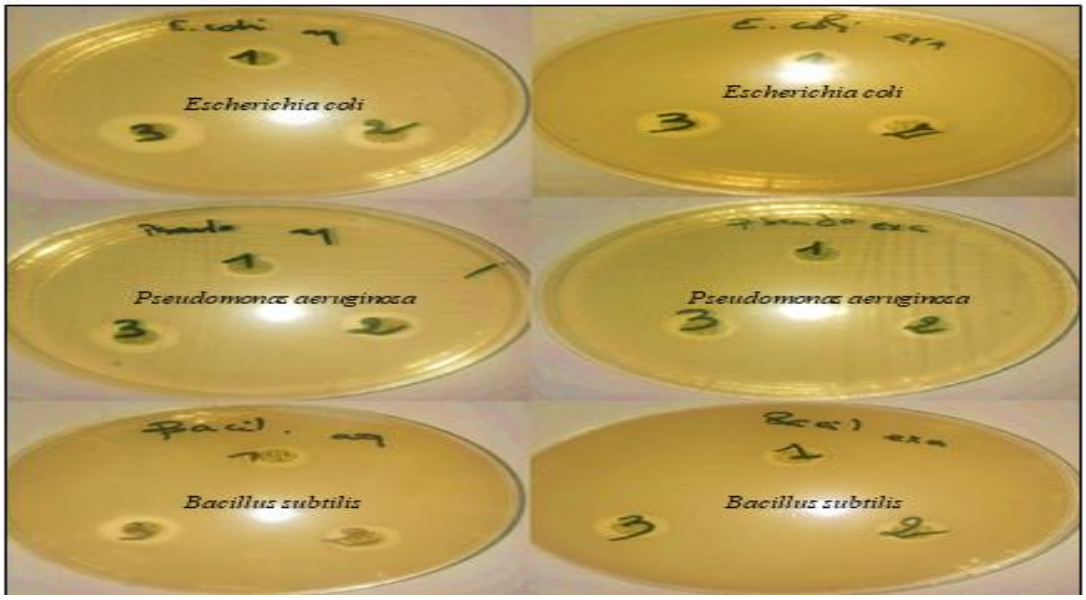

Figure 7. Antibacterial activity of silver nanoparticle against *Escherichia coli*, *Pseudomonas aeruginosa* and *Bacillus subtilis.*

Table 1. Antibacterial activity of silver nanoparticles against *(E. coli , P.aeruginosa* and *B. subtilis)*

	Iinhibition Zone (mm)		
[AgNPs] (µg mL^{-1})	***Escherichia coli***	***Pseudomonas aeruginosa***	***Bacillus subtilis***
200	13	12	10
400	14	13	9
600	15	13	12
800	20	14	12
1000	22	15	14

DOI: http://dx.doi.org/10.32571/ijct.1507097 E-ISSN: 2602-277X

We observe that the different strains of studied bacteria react differently, even if they are two strains of the same gram of bacteria. Among all the samples depicted the largest inhibition zone is noted for the highest concentration (1000 µg/mL) of nanoparticles.[48] Ag NPs show a higher antimicrobial efficacy at the lowest concentration (200 µg/mL) with the different bacteria tested due to the phytoconstituents that mediated the synthesized AgNPs. Previous studies like Sijo Francis *et al*[49] use *Elephantopus scaber* in green synthesis of AgNPs, they found out that the dimeter of the inhibition zone was 16–24 mm against the tested bacterial strains : *B. subtilis, L. lactis, P. fuorescens and P. aeruginosa*. The team explain this results by the presence of phytochemicals flavonoids, alkaloids and polyphenols in the aqueous plant extract that capped the silver nanoparticles. AgNPs can penetrate through the cell wall and cause structural changes by interacting with sulphur and phosphorous containing biomolecules. B. Ajitha *et al*.[50] investigated the use of *Phyllanthus amarus* leaf extract in AgNPs. They found that the inhibition zone diameter ranged from 6 to 11 mm against tested bacterial strains, including *E. coli*, *Pseudomonas* spp., *Bacillus* spp., and *Staphylococcus* spp. Based on antibacterial studies, the authors explained that the bactericidal properties of AgNPs is primarily attributed to the formation of silver cations (Ag^+), which attach to the bacterial cell wall through electrostatic attraction than penetrate in the bacteria.
The detailed mechanism of antimicrobial action of silver NPs is still not widely known. Anupam Roy *et al* in their review explain three well-defined mechanisms: the first step is the damage in the cell wall and membrane, the second step is NPs intracellular diffusion and damage, and the last step is the oxidative stress.[51]

4. CONCLUSION

The biosynthesis of AgNPs via aqueous extract is an effortless, rapid, low-cost and clean process. The AgNPs prepared as described have proved an important antimicrobial activity against both gram-negative and gram-positive bacteria. This strong antimicrobial activity, coupled with the nanometric size and spherical shape of the synthesized nanoparticles, spots them as promising candidates for diverse medical and antimicrobial applications, giving promising solutions without risks.

Moreover, this study substantiates the efficacy of the aqueous extract-mediated bio-reduction method for the controlled fabrication of nanostructures. The demonstrated antimicrobial potency and biocompatibility of AgNPs underscore their potential utility across multifaceted domains, encompassing biomedical, food, and anticancer applications. Particularly noteworthy is the potential future exploitation of AgNPs as a strategic response to the escalating challenge of antibiotic resistance, thereby contributing to the development of effective and sustainable solutions in the realm of nanotechnology.

ACKNOWLEDGEMENTS

The authors are grateful to the direction of hygiene Laboratory of Blida, Algeria for antibacterial activity

Conflict of interest

Authors declare that there is no a conflict of interest with any person, institute, company, etc.

REFERENCES

1. Abbasi, Z.; Feizi, S.; Taghipour, E.; Ghadam, P., Green Process Synth 2017, 6 (5), 477-485.

2. Abdallah, R.; Hammoda, H.; Radwan, M.; El-Gazzar, N.; Wanas, A.; Elsohly, M.; el demellawy, M.; AbdelRahman, N.; Sallam, S. Nat Pro Res 2020, 35, 1-4.

3. Ahmad, N.; Sharma, S.; Singh, V. N.; Shamsi, S. F.; Fatma, A.; Mehta, B. R. Biotechnol Rese Int 2011, 2011, 454090.

4. Ahmed, S.; Saifullah; Ahmad, M.; Swami, B. L.; Ikram, S. J radiat res appl sci 2016, 9 (1), 1-7.

5. Alam, T.; Purnomo, F. O.; Tanjung, A. J Kim Sains Apl 2021, 24 (3), 70-76.

6. Alsamhary, K. I, Saudi J. Biol. Sci 2018, 27(8), 2185-2191.

7. Anastas, P.; Eghbali, N. Chem Soc rev 2010, 39 1, 301-12.

8. Annamalai, J.; Ummalyma, S. B.; Pandey, A.; Bhaskar, T. Environ Sci Pollut R 2021, 28 (36), 49362-49382.

9. B. Ajitha, Y. A. K. Reddy, H.-J. Jeon and C. W. Ahn, Adv. Powder Technol., 2018, 29, 86–93

10. Baali, N.; Mezrag, A.; Bouheroum, M.; Benayache, F.; Benayache, S.; Souad, A. Med Chem 2020, 19 (2), 128-139.

11. Chiang, C. S.; Lin, Y. J.; Lee, R.; Lai, Y. H.; Cheng, H. W.; Hsieh, C. H., Nat Nanotechnol, 2018 13(2), 746–754.

12. Dalmarco, J. B.; Dalmarco, E. M.; Koelzer, J.; Pizzolatti, M. G. Int J Green Pharm 2010, 4 (2),108-114.

DOI: http://dx.doi.org/10.32571/ijct.1507097 **E-ISSN: 2602-277X**

13. Erenler, R., Dag, B.. Inorg and Nano-Metal Chem 2021, 52(4), 485–492.

14. Erenler, R.; Geçer, E. N.; Nusret, G.; Yanar, D. Int J Chem Technol 2021, 5 (2), 141-146.

15. Erenler, R.; Geçer, E. N.; Bozer, B. M. Int J Chem Technol 2022, 6 (2), 142-146.

16. Foo, L. Y.; Newman, R.; Waghorn, G.; McNabb, W. C.; Ulyatt, M. J. Phytochemistry 1996, 41 (2), 617-624.

17. Francis, S.; Joseph, S.; Koshy, E. P. ; Mathew, B. Artif. Cells, Nanomed., Biotechnol., 2018, 46, 795–804.

18. Fumić, B.; Jug, M.; Zovko Končić, M. Croat Chem Acta 2019, 92(3), 369-377

19. Gade, A.; Gaikwad, S.; Tiwari, V.; Yadav, A.; Ingle, A.; Rai, M. Curr. Nanosci 2010, 6 (4), 370-375.

20. Ganesan, R.; Narasimhalu, P.; Joseph, A. I. J.; Pugazhendhi, A. Int J Energ Res 2021, 45 (12), 17378-17388.

21. Gardea-Torresdey, J. L.; Gomez, E.; Peralta-Videa, J. R.; Parsons, J. G.; Troiani, H.; Jose-Yacaman, M. Langmuir 2003, 19 (4), 1357-1361.

22. Hasan, K. F.; Xiaoyi, L.; Shaoqin, Z.; Horváth, P. G.; Bak, M.; Bejó, L.; Sipos, G.; Alpár, T., Heliyon 2022, 8 (12),1-26.

23. Huang, J.; Lin, L.; Li, Q.; Sun, D.; Wang, Y.; Lu, Y.; He, N.; Yang, K.; Yang, X.; Wang, H.; Wang, W.; Lin, W. Ind Eng Chemis Res 2008, 47 (16), 6081-6090.

24. Ito, A.; Shinkai, M.; Honda, H.; Kobayashi, T.,J, biosci and bioeng 2005, 100(1), 1-11

25. Jain, H. Daima, S. Kachhwala, S. Kothari,, Digest J Nano and Biostr 2009, 4(1), 557-563 .

26. Jang, S.; Rahman, M. Appl Phys A 2021, 127, 1-14.

27. Javed, B.; Ikram, M.; Farooq, F.; Sultana, T.; Mashwani, Z.-u.-R.; Raja, N. I. App Microbol Biot 2021, 105, 2261-2275.

28. Kaegi, R.; Voegelin, A.; Sinnet, B.; Zuleeg, S.; Hagendorfer, H.; Burkhardt, M.; Siegrist, H. Environ Sci . technol 2011, 45 (9), 3902-3908.

29. Kaviya, S.; Santhanalakshmi, J.; Viswanathan, B.; Muthumary, J.; Srinivasan, K. Spectrochim Acta A 2011, 79 (3), 594-598.

30. Liu, Y.; Lopes, R. P.; Lüdtke, T.; Di Silvio, D.; Moya, S.; Hamon, J.-R.; Astruc, D. Inorg Chem Front 2021, 8 (13), 3301-3307.

31. Martinez-Gutierrez, F.; Olive, P. L.; Banuelos, A.; Orrantia, E.; Nino, N.; Sanchez, E. M.; Ruiz, F.; Bach, H.; Av-Gay, Y. Nanomed Nanotechnol Bio Med 2010, 6 (5), 681-688.

32. Mitchell, M. J.; Billingsley, M. M.; Haley, R. M.; Wechsler, M. E.; Peppas, N. A.; Langer, R., Nat. reviews drug disc 2021, 20(2), 101-124.

33. Morris, P.; Carter, E. B.; Hauck, B.; Lanot, A.; Theodorou, M. K.; Allison, G. Planta 2021, 253, 1-15.

34. Paramelle, D.; Sadovoy, A.; Gorelik, S.; Free, P.; Hobley, J.; Fernig, D. G. Analyst 2014, 139 (19), 4855-4861.

35. Pareek, V.; Bhargava, A.; Gupta, R.; Jain, N.; Panwar, J. Adv.Sci.Eng. Med 2017, 9 (7), 527-544.

36. Rodrigues, T. S.; da Silva, A. G.; Camargo, P. H. J.Mater.Chem A 2019, 7 (11), 5857-5874.

37. Roy, A.; Bulut, O.; Some, S.; Mandal, A. K.; Yilmaz, M. D. RSC advances 2019, 9 (5), 2673-2702.

38. Salehi, S.; Shandiz, S. A. S.; Ghanbar, F.; Darvish, M. R.; Ardestani, M. S.; Mirzaie, A.; Jafari, M. Int j nanomed 2016, 11, 1835-46

39. Saratale, R. G., Shin, H. S., Kumar, G., Benelli, G., Kim, D. S., & Saratale, G. D. Artificial Cells, Nanomed, and Biotech 2017, 46(1), 211–222.

40. Shankar, S. S.; Ahmad, A.; Sastry, M. Biotechnol prog 2003, 19 (6), 1627-1631.

41. Shankar, T.; Karthiga, P.; Swarnalatha, K.; Rajkumar, K. Resour Efficient Technol 2017, 3 (3), 303-308.

42. Srikar, S. K.; Giri, D. D.; Pal, D. B.; Mishra, P. K.; Upadhyay, S. N. Green Sustain Chem 2016, 6 (1), 34-56.

DOI: http://dx.doi.org/10.32571/ijct.1507097 **E-ISSN: 2602-277X**

43. Stockman, M. I., Phys. Tod 2011, 64(2), 39-44.

44. Sudha, A.; Jeyakanthan, J.; Srinivasan, P. Resour Efficient Technol 2017, 3 (4), 506-515.

45. Vivekanandhan, S.; Schreiber, M.; Mason, C.; Mohanty, A. K.; Misra, M. Colloids Sur f B 2014, 113, 169-175.

46. Wang, C.; Kim, Y. J.; Singh, P.; Mathiyalagan, R.; Jin, Y.; Yang, D. C. Artif cells nanomed biotechnol 2016, 44 (4), 1127-1132.

47. Wang, Edina ,C.; Wang, Andrew ,Z. Integ. biolo 2014, 6(1), 9-26.

48. Xia, Q.; Zhang, Y.; Li, Z.; Hou, X.; Feng, N., Acta Pharma. Sinica B 2019, 9(4), 675-689.

49. Yerlikaya, S.; Baloglu, M. C.; Diuzheva, A.; Jekő, J.; Cziáky, Z.; Zengin, G. J pharm biomed anal 2019, 174, 286-299.

50. Youssef, A.; El-Swaify, Z.; Maaty, D.; Youssef, M.; Garrido, G. J. Pharm. Pharmacogn. Res 2020, 8, 537-548.